

Modeling of reduced secondary electron emission yield from a foam or fuzz surface

Cite as: J. Appl. Phys. **123**, 023302 (2018); <https://doi.org/10.1063/1.5008261>

Submitted: 04 October 2017 . Accepted: 11 December 2017 . Published Online: 10 January 2018

Charles Swanson , and Igor D. Kaganovich 

COLLECTIONS

 This paper was selected as Featured



View Online



Export Citation



CrossMark

ARTICLES YOU MAY BE INTERESTED IN

[Tutorial: Novel properties of defects in semiconductors revealed by their vibrational spectra](#)
Journal of Applied Physics **123**, 161561 (2018); <https://doi.org/10.1063/1.5011036>

[Modeling of reduced effective secondary electron emission yield from a velvet surface](#)
Journal of Applied Physics **120**, 213302 (2016); <https://doi.org/10.1063/1.4971337>

[Tutorial: Physics and modeling of Hall thrusters](#)
Journal of Applied Physics **121**, 011101 (2017); <https://doi.org/10.1063/1.4972269>

Journal of
Applied Physics

SPECIAL TOPIC:
Polymer-Grafted Nanoparticles

Submit Today!

Modeling of reduced secondary electron emission yield from a foam or fuzz surface

Charles Swanson and Igor D. Kaganovich

Princeton Plasma Physics Laboratory, Princeton University, Princeton, New Jersey 08543, USA

(Received 4 October 2017; accepted 11 December 2017; published online 10 January 2018)

Complex structures on a material surface can significantly reduce the total secondary electron emission yield from that surface. A foam or fuzz is a solid surface above which is placed a layer of isotropically aligned whiskers. Primary electrons that penetrate into this layer produce secondary electrons that become trapped and do not escape into the bulk plasma. In this manner the secondary electron yield (SEY) may be reduced. We developed an analytic model and conducted numerical simulations of secondary electron emission from a foam to determine the extent of SEY reduction. We find that the relevant condition for SEY minimization is $\bar{u} \equiv AD/2 \gg 1$ while $D \ll 1$, where D is the volume fill fraction and A is the aspect ratio of the whisker layer, the ratio of the thickness of the layer to the radius of the fibers. We find that foam cannot reduce the SEY from a surface to less than 0.3 of its flat value. *Published by AIP Publishing.* <https://doi.org/10.1063/1.5008261>

I. INTRODUCTION

Secondary electron emission (SEE) from dielectric and metallic surfaces can significantly change the electric potential profiles and fluxes near that surface. In low-temperature plasma applications, SEE may limit the total throughput. Examples are RF amplifiers,¹ particle accelerators, and Hall thrusters.^{2–4} Texturing the geometry of the walls of the device to reduce the secondary electron yield (SEY) is an area of active research. Examples of recent subjects of research are triangular grooves,^{5–8} oxides,⁹ dendritic structures,¹⁰ micro-porous structures,¹¹ and fibrous structures.

Such fibrous structures can include velvet, feathers, and foam. Fibrous structures are layers of whiskers grown onto a surface. In a velvet, the whiskers are all aligned in one direction, usually normal to the surface.^{4,12–14} In a previous publication,¹⁴ we predicted that velvets are well-suited to minimizing SEY from a distribution of primary electrons that are normally incident. In this case, the reduction factor can be $<10\%$.

Note: In this paper, when we write “reduced by $n\%$,” we mean that $\gamma \rightarrow (1 - \frac{n}{100\%})\gamma$ and when we write “reduction factor of $n\%$,” we mean that $\gamma \rightarrow \frac{n}{100\%}\gamma$.

In a feathered surface, the whiskers are also aligned normally and have smaller whiskers grown onto their sides. In a previous publication,¹⁵ we predicted that these secondary whiskers serve to reduce SEY from more shallowly incident primary electrons and allow a more isotropic reduction in SEY.

In foam, and closely related fuzz, the whiskers are isotropically aligned, producing a random layer of criss-crossing whiskers.^{13,16,17} The SEY from fuzz/foam is of interest to the low-temperature plasma modeling community because it is expected to behave more isotropically than the uniformly aligned fibers of velvet. The SEY from fuzz/foam is of interest to the high-temperature plasma modeling community because tungsten fuzz is spontaneously generated in the tungsten divertor region of Tokamak plasma confinement vessels.

Recent experiments on this self-generated tungsten fuzz reports SEY reduction factors of 40%–60% and little dependence on the primary angle of incidence.¹⁷

Copper fuzz/foam was simulated using a Monte-Carlo algorithm recently.¹³ The geometry used was a “cage” geometry consisting of normally aligned whiskers and perfectly regular, rectangularly placed, horizontal whiskers. Using this approximation and geometrical values taken from experimental characterization of real foams, the reduction factor was calculated to be 70%.

In this paper, we report the results of numerical simulations of SEY from a foam surface. Furthermore, we apply a simplified analytic model to explain the results. The numerical values in this paper will be given assuming a carbon graphite surface. However, according to the analytical model, the SEY reduction is not dependent on material.

II. NUMERICAL MODEL

We performed a Monte Carlo calculation of the SEY of a foam surface. We used the same simulation tool that was previously used to simulate SEY from velvet and was benchmarked against analytical calculations.¹⁴

We numerically simulated the emission of secondary electrons by using the Monte Carlo method, initializing many particles and allowing them to follow ballistic, straight-line trajectories until they interact with the surface. The surface geometry was implemented as an isosurface, a specially designed function of space that gives correct structure. The SEY of a particle interacting with a flat surface was assumed to follow the empirical model of Scholtz¹⁸

$$\gamma(E_p, \theta) = \gamma_{max}(\theta) \times \exp \left[- \left(\frac{\ln[E_p/E_{max}(\theta)]}{\sqrt{2}\sigma} \right)^2 \right]. \quad (1)$$

Secondary electrons were assumed to be emitted with probability weighted linearly with normal velocity component (cosine-law emission).¹⁹

For parameters in the model $\gamma_{max}(\theta)$, E_p , $E_{max}(\theta)$, σ , we used those of graphite,²⁰ assuming structures are carbon based. The form of the angular dependence $\gamma_{max}(\theta)$, $E_{max}(\theta)$ is taken from Vaughan²¹

$$\gamma_{max}(\theta) = \gamma_{max0} \left(1 + \frac{k_s \theta^2}{2\pi} \right), \quad (2)$$

$$E_{max}(\theta) = E_{max0} \left(1 + \frac{k_s \theta^2}{\pi} \right).$$

The parameters used were $\gamma_{max0} = 1.2$, $E_{max0} = 325$ eV, $\sigma = 1.6$, $k_s = 1$.

We initialized the primary electrons with an energy of 350 eV. True secondary electrons, elastically scattered electrons, and inelastically scattered electrons were taken into consideration. This energy was chosen to demonstrate the effect of multiple generations of secondary electrons (tertiary electrons). As our analytical model in Sec. IV does not include tertiary electrons, 350 eV can be considered a worst-case scenario for applicability. For more discussion on the model and its implementation in the Monte Carlo calculations, see our previous paper on SEE from velvet.¹⁴

Foam was implemented as a collection of whiskers. The whiskers within one simulation all had the same radii. Whisker radius, height of the simulation volume, and number of whiskers were the free parameters of the simulation. The whiskers were as long as to fit within the simulation volume. An example of such a surface is depicted in Fig. 1.

The isosurface function that represents one whisker was radial distance from its axis to the inverse 3rd power. The function of the collection of whiskers was many such

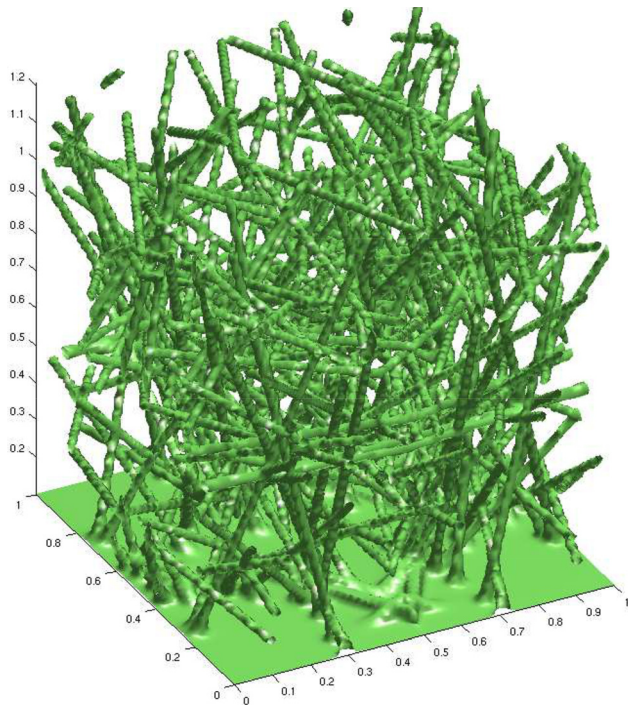


FIG. 1. Rendering of an example of the foam surface used in this paper. This foam had 80 fibers, aspect ratio $A = 10$, volume fill fraction $D = 4.3\%$, and foam parameter $\bar{u} = 2.2$. The absolute length scale is not defined for our analytic model.

isosurface functions summed. The inverse 3rd power function falls quickly enough at large radii that whiskers next to each other did not deform each other's shapes. Whisker starting locations were chosen randomly, uniform in space, and axis alignments were chosen randomly, uniform in solid angle.

In commercially available foams, foam whiskers extend a finite distance rather than as long as fits within the foam layer. This is different from our Monte Carlo calculations. In Sec. IV, we find that the SEY from a foam surface depends only on local parameters. Because of this, we expect our calculations to be applicable to foams with finite whisker length.

Real foam whiskers can be grown to have any radius. This paper assumes that the radius is large compared to the electron penetration length into carbon, $r \gg 10$ nm. Other than this criterion, our models consider only dimensionless quantities such as packing density and aspect ratio, so absolute length scales are not important. Our models find a SEY that is only dependent on A and D , the aspect ratio and packing fraction.

III. ANALYTIC MODEL

To support the numerical results, we formulated an analytic model of secondary electron emission from foam. This analytic model is an extension of a model published in our previous paper.¹⁴ While our previous model considered a field of uniformly aligned whiskers ($\hat{a} = \hat{z}$), we consider a field of randomly aligned whiskers (\hat{a} isotropic). Here, \hat{a} is the direction of the whisker axis.

As in the velvet model, we consider only one generation of secondary electrons. No tertiary electrons will be considered.

As in the velvet model, we consider secondary electron emission from three surfaces: The top of the foam, the sides of the whiskers, and the bottom surface onto which the whiskers are grown. These three cases are depicted in Fig. 2.

$$\gamma_{eff} = \gamma_{top} + \gamma_{bottom} + \gamma_{sides}. \quad (3)$$

The reduction from SEY can be interpreted as the probability that a secondary electron will escape from the whisker layer

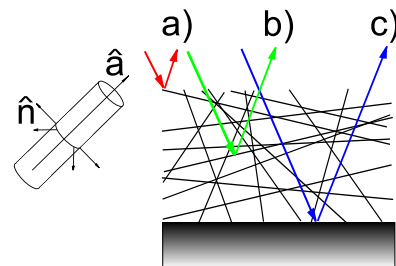


FIG. 2. Schematic example of the three categories of SEE: (a) γ_{top} from primary electrons that impact top of the structure, (b) γ_{sides} from primary electrons that impact the whisker sides, and (c) γ_{bottom} from primary electrons that impact the bottom surface. Also depicted at left: Whisker axis \hat{a} and normal vectors \hat{n} .

$$\gamma_{\text{eff}} = \gamma P(\text{escape}). \quad (4)$$

Written as probabilities

$$\begin{aligned} \gamma_{\text{eff}} = & \gamma P(\text{escape}|top) \cdot P(top) \\ & + \gamma P(\text{escape}|bottom) \cdot P(bottom) \\ & + \langle \gamma \rangle P(\text{escape}|sides) \cdot P(sides), \end{aligned} \quad (5)$$

where $\langle \gamma \rangle$ in the third term will be explained in this section.

We will determine these probability values using the assumption that electrons inside a whisker layer hit the whiskers with uniform probability per unit distance traveled perpendicular to the whiskers' axes. If the whiskers have radius r and areal density (whiskers per unit area, where area is defined perpendicular to the axis) n , the probability of intersection with a whisker is

$$P(\text{hit}) = 2rn dS_{\perp}, \quad (6)$$

where dS_{\perp} is the distance traveled perpendicular to the axis. If the whiskers are aligned along \hat{a} , this becomes

$$P(\text{hit}) = 2rn \frac{\sqrt{1 - \hat{v} \cdot \hat{a}^2}}{\hat{v} \cdot \hat{z}} dz, \quad (7)$$

where z is the direction normal to the solid surface and \hat{v} is the direction of primary electron incidence. This equation is linear with density n of whiskers. Different populations of whiskers 1, 2 simply add

$$P_{1+2}(\text{hit}) = 2rn_1 \frac{\sqrt{1 - \hat{v} \cdot \hat{a}_1^2}}{\hat{v} \cdot \hat{z}} dz + 2rn_2 \frac{\sqrt{1 - \hat{v} \cdot \hat{a}_2^2}}{\hat{v} \cdot \hat{z}} dz. \quad (8)$$

Since \hat{a} is isotropic, $l \equiv \hat{a} \cdot \hat{v}$ is uniformly distributed. Thus in a field of infinitely many infinitesimally dense fields of isotropically aligned whiskers, the probability of hitting one is

$$P(\text{hit}) = 2rn \frac{dz}{\mu} \int_{-1}^1 dl \frac{\sqrt{1 - l^2}}{2} = \frac{\pi}{2} rn \frac{dz}{\mu}, \quad (9)$$

where $\mu \equiv \hat{v} \cdot \hat{z}$.

The probability that an electron will traverse Δz without having hit a whisker is this value integrated over z

$$P(\Delta z) = e^{-\frac{\pi}{2} rn \frac{\Delta z}{\mu}} = e^{-\frac{\bar{u} \Delta z}{h}}. \quad (10)$$

We have discovered the important parameter to describe the SEY reduction from a foam, $\bar{u} \equiv \frac{\pi}{2} rhn = AD/2$, where A is the aspect ratio $A \equiv hr$ and D is the volume fill density. \bar{u} is a measure of how much whisker there is: the more dense, or long, or wide the whiskers, the higher \bar{u} . It is related ($\bar{u} = \frac{\pi}{4} u$) to the parameter u found for velvet, with the differences in geometry accounting for the numerical coefficient.¹⁴

A. γ_{top}

If a primary electron hits the top of the foam region, where the foam meets the vacuum, all secondary electrons will be freely conducted to the bulk ($P(\text{escape}|top) = 1$). A primary electron hits the top with probability D , as this is also the surface fill fraction ($P(top) = D$)

$$\gamma_{\text{top}} = D\gamma. \quad (11)$$

B. γ_{bottom}

The SEY from the bottom surface is

$$\gamma_{\text{bottom}} = \gamma P(\text{escape}|bottom) P(bottom). \quad (12)$$

The probability that a primary electron reaches the bottom surface can be derived from Eq. (10)

$$P(bottom) = e^{-\frac{\bar{u}}{h}}. \quad (13)$$

The probability that a secondary electron escapes after being emitted from the bottom depends on its emitted polar angle and in integrated form is

$$P(\text{escape}|bottom) = \int_0^1 d\mu_2 P(\text{escape}|\mu_2, \text{bottom}) P(\mu_2), \quad (14)$$

where $P(\mu_2) d\mu_2$ is the probability density function (PDF) of $\mu_2 = \cos \theta_2$, the polar angle of the secondary electron. Assuming a cosine distribution for the probability of polar angles of secondary electrons,¹⁹ $P(\mu_2) = 2\mu_2$.

$P(\text{escape}|\mu_2, \text{bottom})$ can also be determined from Eq. (10), yielding a final bottom SEY of

$$\gamma_{\text{bottom}} = 2\gamma(1 - D) \int_0^1 d\mu_2 \mu_2 e^{-\left(\frac{1}{\mu} + \frac{1}{\mu_2}\right)\bar{u}}. \quad (15)$$

C. γ_{sides}

The procedure is similar for γ_{sides} , except that the secondary electron may be emitted at any z value from 0 to h

$$\gamma_{\text{sides}} = \langle \gamma \rangle (1 - D) \int_0^h dz P(\text{escape}|z) P(z). \quad (16)$$

Again $P(z) dz$, the PDF that an electron hit within dz may be derived from Eq. (10).

$\langle \gamma \rangle$ is necessary as, according to the empirical model of Vaughan,²¹ SEY from a primary electron which is shallowly incident is larger than SEY from a primary electron which is normally incident. According to Eq. (2) and the value of $k_s = 1$ of a smooth surface, the average SEY from isotropically aligned surface elements will be larger than that of the flat value by

$$\langle \gamma \rangle / \gamma = \int_0^1 d(\cos \theta) 2 \cos \theta \left(1 + \frac{\theta^2}{2\pi} \right) \approx 1.12. \quad (17)$$

Keeping explicit the dependence on μ_2 , Eq. (16) may be written in the form

$$\gamma_{\text{sides}} = \langle \gamma \rangle (1 - D) \int_0^1 d\mu_2 \int_0^1 \frac{z}{h} d\mu_2 \frac{\bar{u}}{\mu} e^{-\bar{u} \left(\frac{1}{\mu} + \frac{1}{\mu_2} \right)} P(\mu_2|\mu). \quad (18)$$

Carrying out the z integration gives

$$\gamma_{\text{sides}} = \langle \gamma \rangle (1 - D) \int_0^1 d\mu_2 \frac{1 - e^{-\bar{u} \left(\frac{1}{\mu} + \frac{1}{\mu_2} \right)}}{1 + \frac{\mu}{\mu_2}} P(\mu_2|\mu). \quad (19)$$

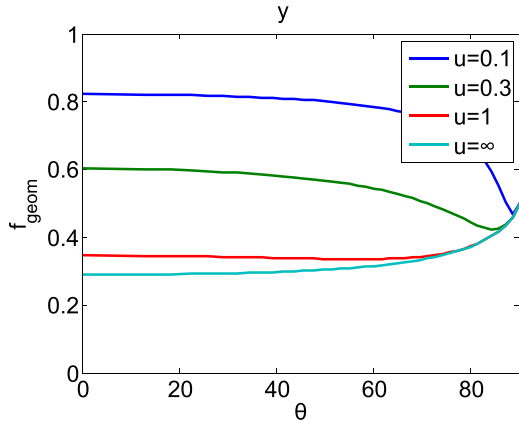


FIG. 3. Results of analytic theory. Total SEY is $\gamma[D + (1 - D)f_{geom}]$.

The function $P(\mu_2|\mu)$ is the probability that a primary electron with polar velocity vector component $\mu = \cos \theta$ produces a secondary electron with polar velocity component $\mu_2 = \cos \theta_2$. Clearly, this depends on where on a fiber this electron hits, and how the fiber is aligned.

To determine this, we appeal to geometrical reasoning. Since \hat{a} , the whisker axes, are isotropically distributed, so too are \hat{n} , the vectors normal to the surface elements on the sides of the whiskers. Because of this, the probability that a primary electron hits a surface element with normal \hat{n} will be linearly weighted by $\hat{v} \cdot \hat{n}$.

Integrating over all surface element normal vectors \hat{n} and leaving out some tedious steps

$$P(\mu_2|\mu) = \frac{4}{\pi} \int_{-1}^1 dm (A_1 \sin \phi_1 + B_1 \phi_1) (A_2 \sin \phi_2 + B_2 \phi_2), \quad (20)$$

$$A_{1,2} = \sqrt{(1 - m^2)(1 - \mu_{1,2}^2)}, \quad B_{1,2} = m\mu_{1,2}$$

$$\phi_{1,2} = \text{Re} \left[\cos^{-1} \left(-\frac{B_{1,2}}{A_{1,2}} \right) \right],$$

where $\text{Re}(x)$ is the real part of x . m is an integration variable, but it may be informative to know that $m = \hat{n} \cdot \hat{z}$.

D. γ_{eff}

Thus, the total SEY from a foam surface is expected to be

$$\gamma_{\text{eff}} = \gamma D + (1 - D) \left[\gamma \int_0^1 d\mu_2 2\mu_2 e^{-\left(\frac{1}{\mu} + \frac{1}{\mu_2}\right)\bar{u}} + \langle \gamma \rangle \int_0^1 d\mu \frac{1 - e^{-\bar{u}\left(\frac{1}{\mu} + \frac{1}{\mu_2}\right)}}{1 + \frac{\mu}{\mu_2}} P(\mu_2|\mu) \right], \quad (21)$$

where $\langle \gamma \rangle$ is defined in Eq. (17) and $P(\mu_2|\mu)$ is defined in Eq. (20). Recall that $\mu = \cos \theta$, where θ is the polar angle. Also recall that D is the volumetric fill ratio and $\bar{u} = AD/2$, where $A = h/r$ the ratio between the whisker layer thickness and the whisker radius.

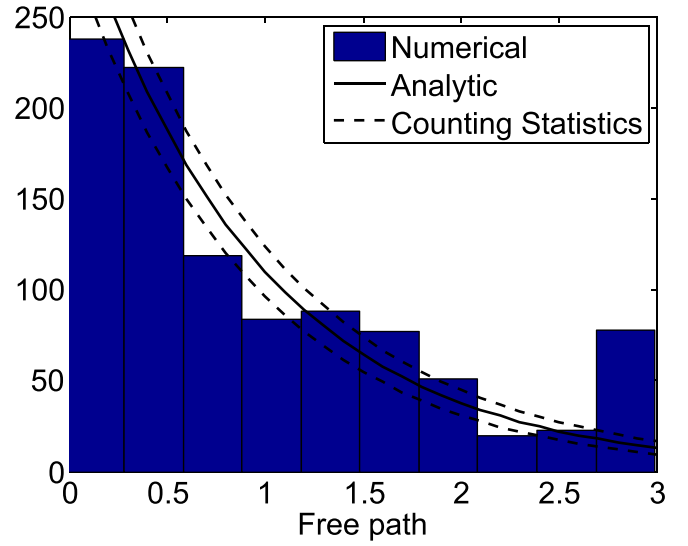


FIG. 4. Mean Free Path comparison: A histogram of free paths calculated during a Monte Carlo simulation compared with the idealized analytic version. Error arises from the counting statistics of both particles and whiskers.

The factor in the square brackets is a function only of \bar{u} and θ . It is plotted in Fig. 3. If the foam is very deep or very dense, \bar{u} is infinity, and there is a limiting case

$$\gamma_{\text{eff}} = \gamma D + (1 - D) \langle \gamma \rangle \int_0^1 d\mu_2 \frac{1}{1 + \frac{\mu}{\mu_2}} P(\mu_2|\mu), \quad (22)$$

which is also plotted in that figure.

For the case of isolated hard-sphere balls of radius r , volume density n , and layer height h , the analytical calculation for SEY is identical. This includes the value of $P(\mu_2|\mu)$. For this case

$$\bar{u}_{\text{ball}} = \pi r^2 n h. \quad (23)$$

IV. RESULTS AND EXPLANATION

The analytic model is based on the assumption that the mean free path is

$$\lambda_{\text{mfp}} = \left(\frac{\pi}{2} r n \right)^{-1}. \quad (24)$$

To verify this, we tabulated the free paths of electrons within the foam layer during a Monte Carlo calculation.

The results are plotted in histogram form in Fig. 4. For this calculation, whisker parameters were $r = 0.005$, $h = 3$, and 160 whiskers were in the simulation volume. This produced a $\bar{u} = 3.2$ and a $\lambda_{\text{mfp}} = 0.94$. The figure indicates that the assumption is qualitatively justified. The excess at a free path of 3 is the result of electrons hitting the bottom surface.

The normalized SEY as a function of primary angle of incidence and the \bar{u} factor is plotted in Fig. 5. Three values of \bar{u} are plotted: The $\bar{u} = 0.1$ run was initialized with whisker layer height $h = 3$, whisker radius $r = 0.0025$, and 10 whiskers total in this volume. The $\bar{u} = 0.4$ run was initialized with whisker layer height $h = 3$, whisker radius

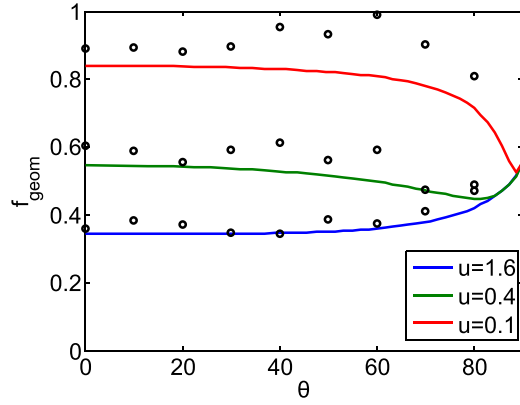


FIG. 5. Results of analytic theory compared to full numerical Monte Carlo model.

$r=0.0025$, and 40 whiskers total in this volume. The $\bar{u} = 1.6$ run was initialized with whisker layer height $h=3$, whisker radius $r=0.005$, and 80 whiskers total in this volume.

We can see from Fig. 5 that the analytic theory consistently underestimates the SEY from a given foam by about 10%. The source of this discrepancy is subsequent generations of secondary electrons. In the analytic model, only one generation of secondary electrons is considered. In Fig. 6, tertiary electrons are disabled. The numerically and analytically calculated results in Fig. 6 are consistent. This discrepancy is at its worst for our chosen value of initial electron energy, 350 eV, as this is near the maximum of the SEY curve.

The behavior of γ at very small \bar{u} can be explained thusly: When there are very few whiskers, or they are very thin, or the whisker layer is very short, the probability of interacting with a whisker is small and so SEY is not reduced by much.

The behavior of γ at shallow angles of incidence ($\theta \rightarrow 90^\circ$) can be explained simply. A primary electron that is shallowly incident will hit a whisker very close to the top of the whisker layer. Because of isotropy of the whisker axes, this electron will have a 0.5 probability of being emitted with velocity in the upward hemisphere and a 0.5 probability of being emitted with velocity in the downward hemisphere.

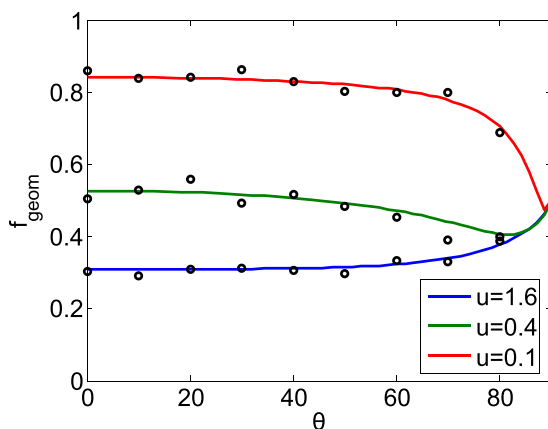


FIG. 6. Results of analytic theory compared to simplified Monte Carlo model consisting of only one generation of secondary electrons and no dependence of SEY on primary angle of incidence.

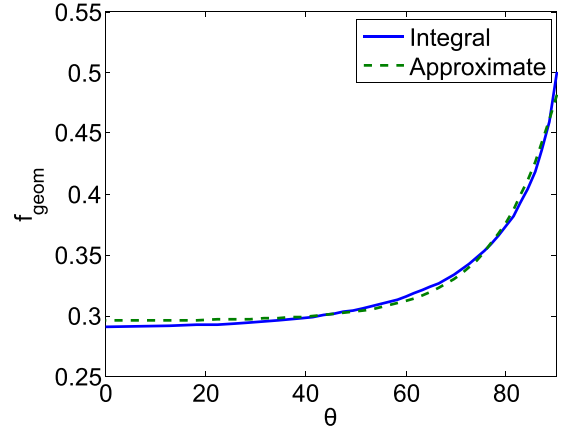


FIG. 7. Results of deep foam limit [Eq. (22)] plotted against its approximate formula [Eq. (25)].

Thus, the SEY from shallow incidence will be reduced by one-half.

The behavior at more normal angles (low θ) at high \bar{u} is very isotropic. There is very little dependence on the angle. This is expected: As \bar{u} increases, almost no electrons penetrate to the bottom surface. If the bottom surface is not relevant, the problem is entirely isotropic.

V. APPROXIMATE FORM

Equation (22), the result in the limit of deep, dense foam, is an important result of this computation. However, it requires a double-integral to obtain numerical values. Because of this, we have determined a simple analytic fit to this line. The fit is

$$\gamma_{eff} \approx C_1 e^{-C_2 \cos \theta} + C_3, \quad (25)$$

where $C_1 = 0.1887$, $C_2 = 4.8196$, and $C_3 = 0.2947$. The root-mean-square error of this approximate formula is 0.46%. This fit is depicted in Fig. 7.

VI. CONCLUSIONS

We calculated the SEY from a foam surface and verified that it is reduced. Furthermore, our calculations support the prediction that SEY from a foam surface will behave more isotropically than from other fibrous surfaces like velvet. We find that foam cannot reduce SEY by more than about 30% of its unsuppressed value. We find that foam does not suppress SEY as much as velvet given the same geometric factors A, D .

ACKNOWLEDGMENTS

The authors would like to thank Yevgeny Raites, who attracted our attention to the SEY of complex surfaces. We would also like to thank Eugene Evans, who suggested the approach of isosurfaces. This work was supported by the U.S. Department of Energy, Office of Fusion Energy Sciences and Program in Plasma Science and Technology.

¹J. R. M. Vaughan, "Multipactor," *IEEE Trans. Electron Devices* **35**, 1172–1180 (1988).

- ²Y. Raitses *et al.*, “Effect of secondary electron emission on electron cross-filed current in $E \times B$ discharges,” *IEEE Trans. Plasma Sci.* **39**, 995 (2011).
- ³H. Wang, M. D. Campanell, I. D. Kaganovich, and G. Cai, “Effect of asymmetric secondary emission in bounded low-collisional $E \times B$ plasma on sheath and plasma properties,” *J. Phys. D: Appl. Phys.* **47**, 405204 (2014).
- ⁴Y. Raitses, I. D. Kaganovich, and A. V. Sumant, “Electron emission from nano- and micro-engineered materials relevant to electric propulsion,” in *33rd International Electric Propulsion Conference, The George Washington University, Washington, DC, USA* (2013), pp. 6–10.
- ⁵G. Stupakov and M. Pivi, “Suppression of the effective secondary emission yield for a grooved metal surface,” in *Proceedings of the 31st ICFA Advanced Beam Dynamics Workshop on Electron-Cloud Effects*, Napa, CA, USA, 19–23 April 2004.
- ⁶L. Wang *et al.*, “Suppression of secondary electron emission using triangular grooved surface in the ILC dipole and wiggler magnets,” in *Proceedings of the Particle Accelerator Conference (PAC 2007)*, Albuquerque, NM, USA, 25–29 June 2007.
- ⁷M. T. F. Pivi *et al.*, “Sharp reduction of the secondary electron emission yield from grooved surfaces,” *J. Appl. Phys.* **104**, 104904 (2008).
- ⁸Y. Suetsugu *et al.*, “Experimental studies on grooved surfaces to suppress secondary electron emission,” in *Proceedings of the IPAC’10*, Kyoto, Japan (2010), pp. 2021–2023.
- ⁹D. Ruzic, R. Moore, D. Manos, and S. Cohen, “Secondary electron yields of carbon-coated and polished stainless steel,” *J. Vac. Sci. Technol.* **20**, 1313 (1982).
- ¹⁰V. Baglin, J. Bojko, O. Grabner, B. Henrist, N. Hilleret, C. Scheuerlein, and M. Taborelli, “The secondary electron yield of technical materials and its variation with surface treatments,” in *Proceedings of EPAC 2000*, 26–30 June 2000, Austria Center, Vienna, pp. 217–221.
- ¹¹M. Ye, W. Dan, and H. Yongning, “Mechanism of total electron emission yield reduction using a micro-porous surface,” *J. Appl. Phys.* **121**(12), 124901 (2017).
- ¹²L. Aguilera *et al.*, “CuO nanowires for inhibiting secondary electron emission,” *J. Phys. D: Appl. Phys.* **46**, 165104 (2013).
- ¹³C. E. Huerta and R. E. Wirz, “Surface geometry effects on secondary electron emission via Monte Carlo modeling,” in *52nd AIAA/SAE/ASEE Joint Propulsion Conference (American Institute of Aeronautics and Astronautics)*, 2016.
- ¹⁴C. Swanson and I. D. Kaganovich, “Modeling of reduced effective secondary electron emission yield from a velvet surface,” *J. Appl. Phys.* **120**(21), 213302 (2016).
- ¹⁵C. Swanson and I. D. Kaganovich, “‘Feathered’ fractal surfaces to minimize secondary electron emission for a wide range of incident angles,” *J. Appl. Phys.* **122**(4), 043301 (2017).
- ¹⁶R. Cimino *et al.*, “Search for new e-cloud mitigator materials for high intensity particle accelerators,” in *Proceedings of the IPAC2014, Dresden, Germany* (2014), pp. 2332–2334.
- ¹⁷M. Patino, Y. Raitses, and R. Wirz, “Secondary electron emission from plasma-generated nanostructured tungsten fuzz,” *Appl. Phys. Lett.* **109**(20), 201602 (2016).
- ¹⁸J. Scholtz *et al.*, “Secondary electron emission properties,” *Phillips J. Res.* **50**, 375 (1996).
- ¹⁹*Vtorichnaya Elektronnaya Emissiya*, edited by I. M. Bronstein and B. S. Fraiman (Nauka Publisher, Moskva, 1969), p. 340 (in Russian).
- ²⁰M. Patino, Y. Raitses, B. Koel, and R. Wirz, “Application of Auger spectroscopy for measurement of secondary electron emission from conducting material for electric propulsion devices,” in *IEPC-2013-320*, The 33rd International Electric Propulsion Conference, The George Washington University, Washington, D.C., USA, 6–10 October 2013.
- ²¹J. Vaughan, “A new formula for secondary emission yield,” *IEEE Trans. Electron Devices* **36**, 1963 (1989).